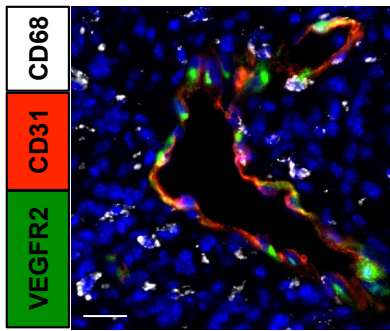
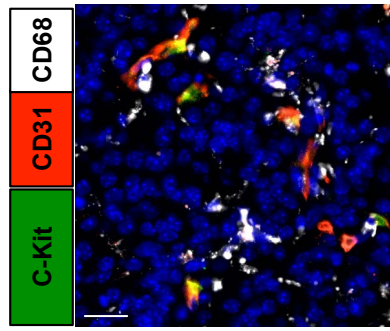


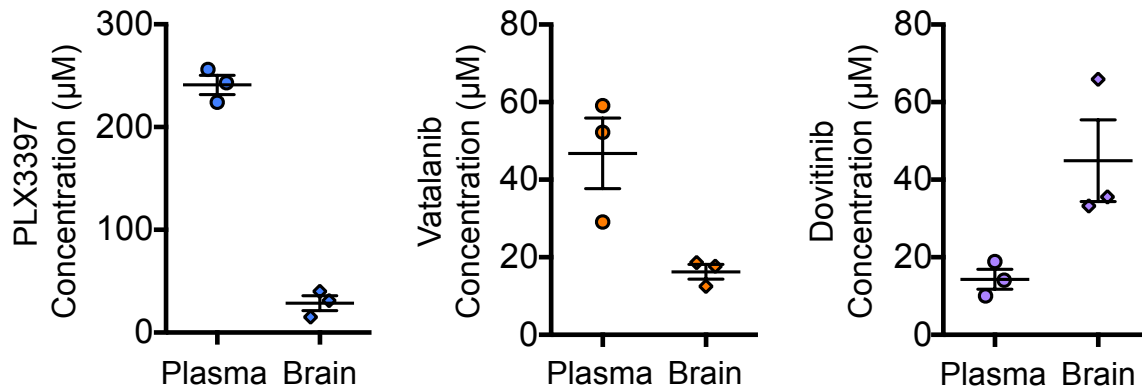
A



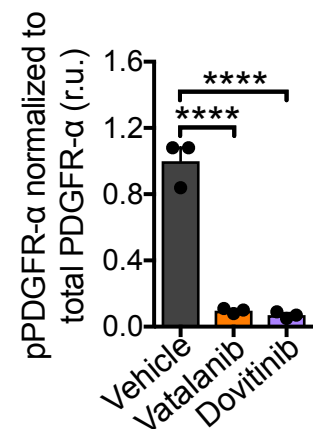
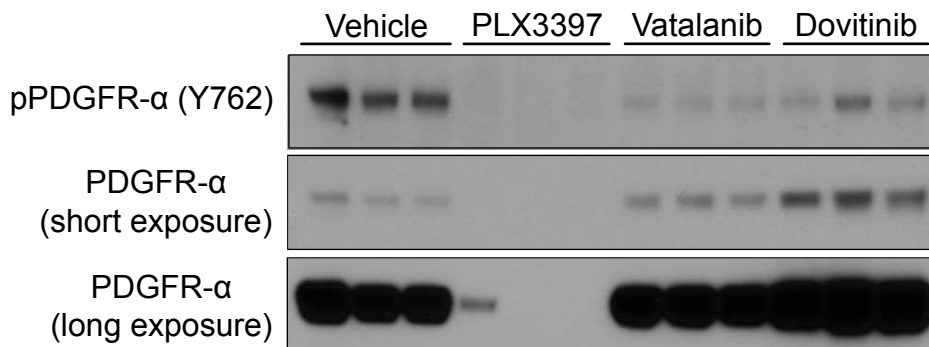
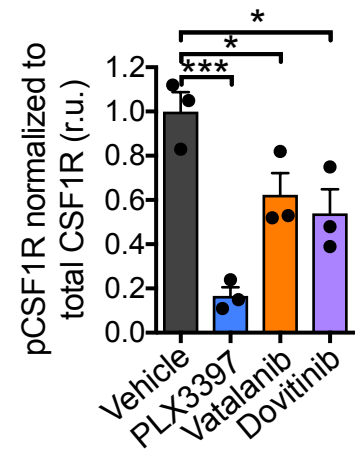
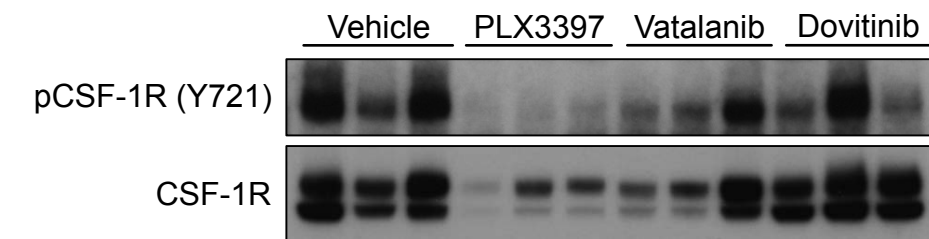
B



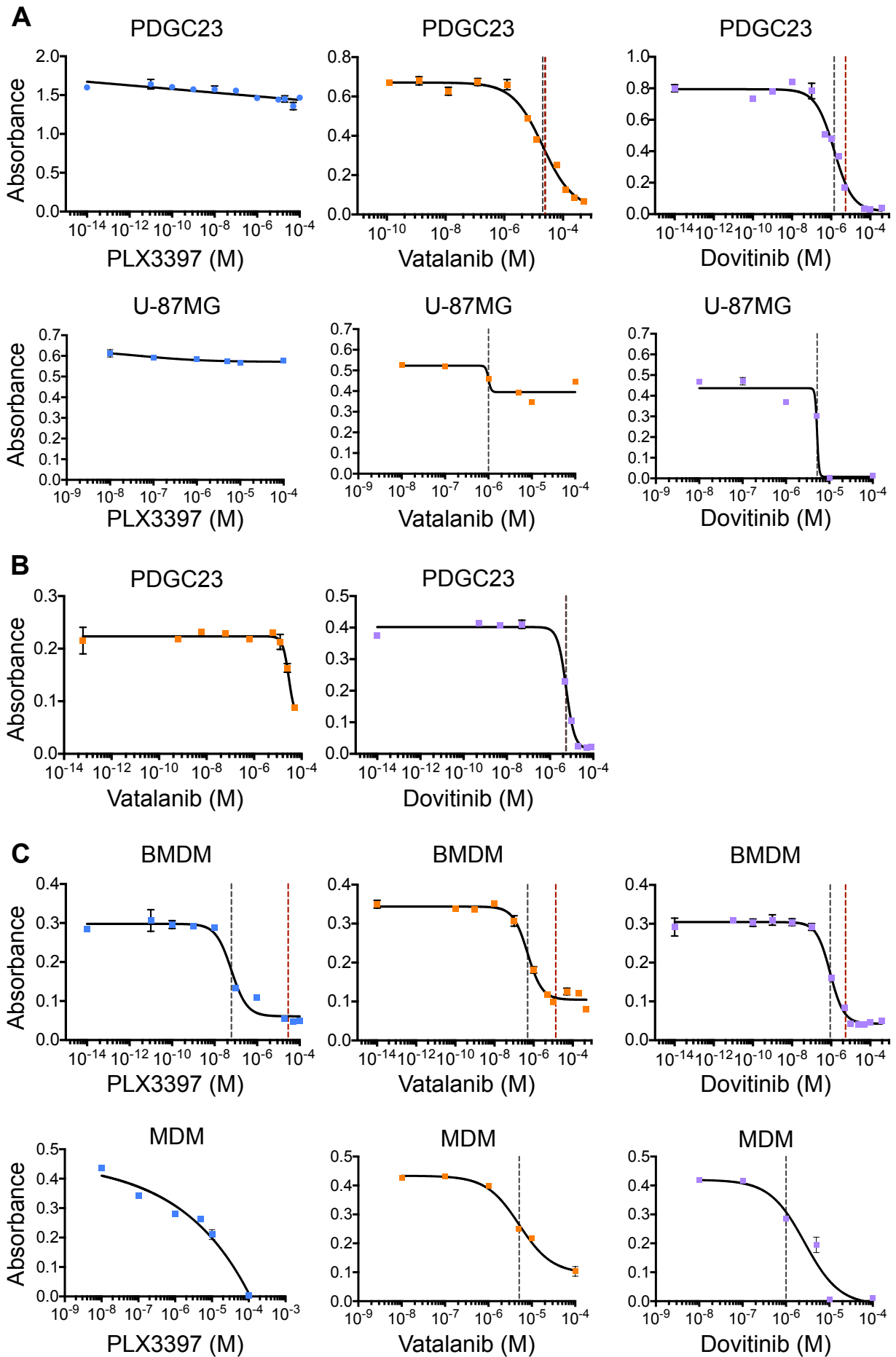
C



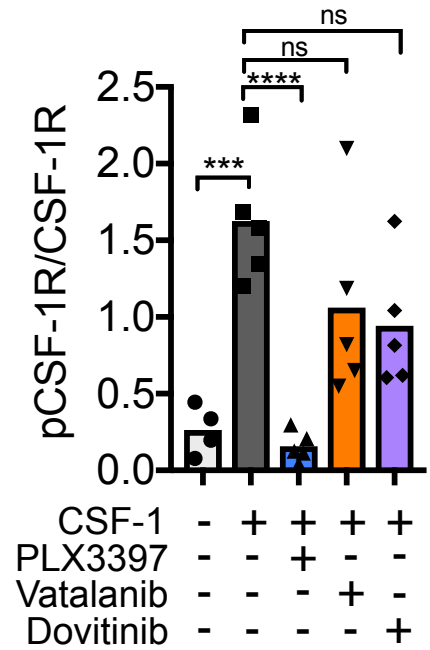
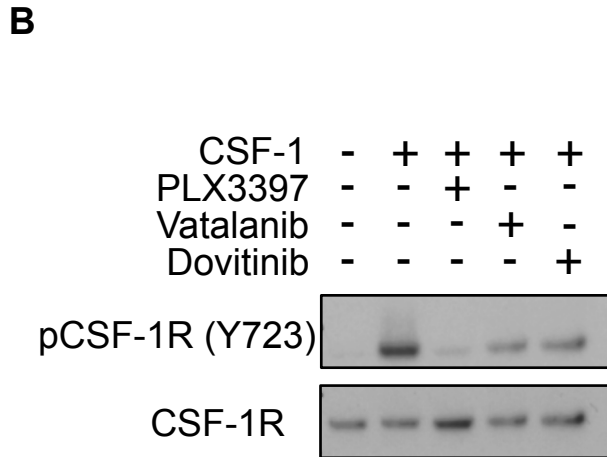
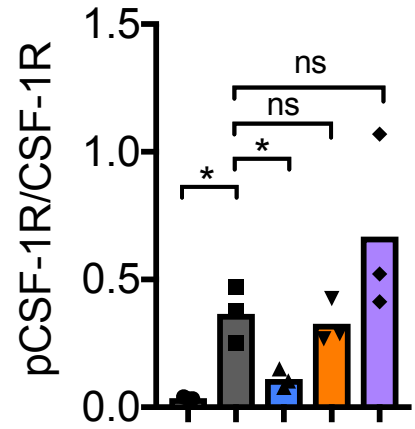
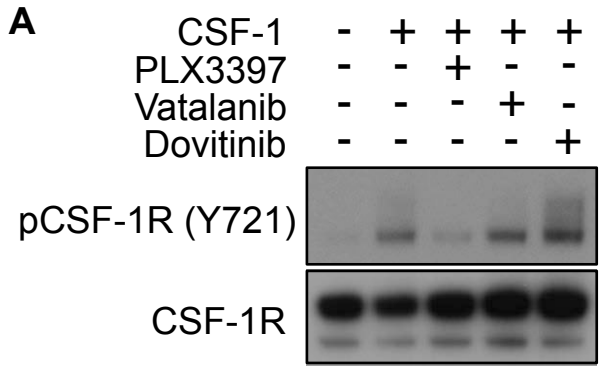
D



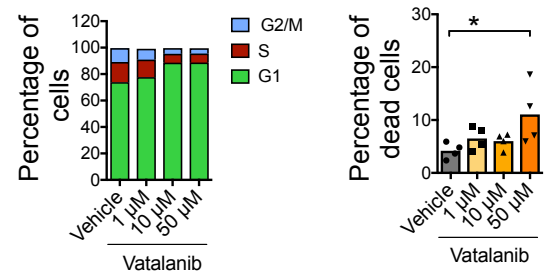
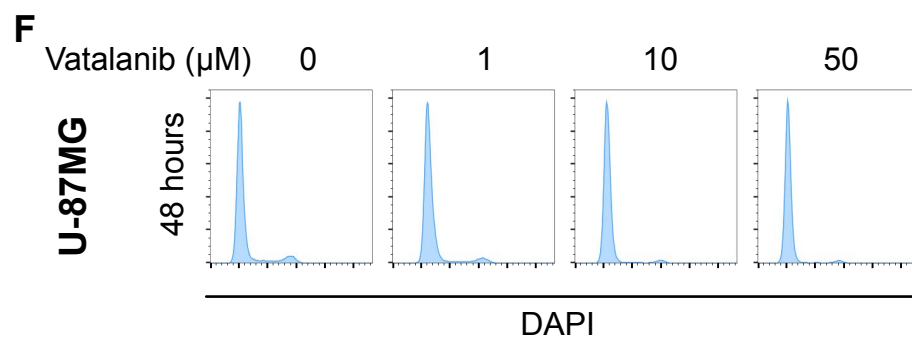
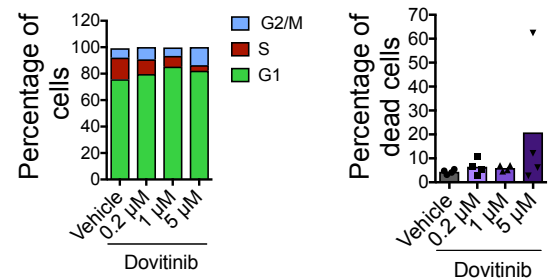
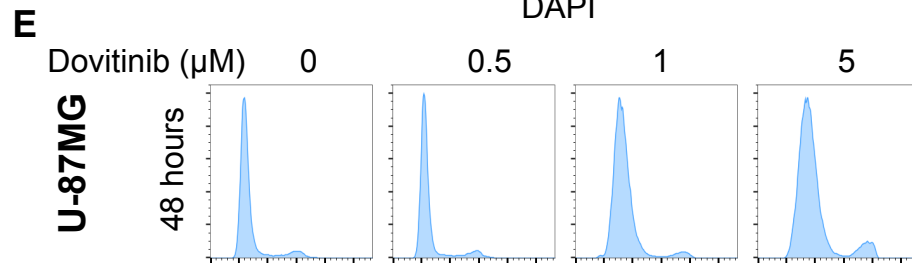
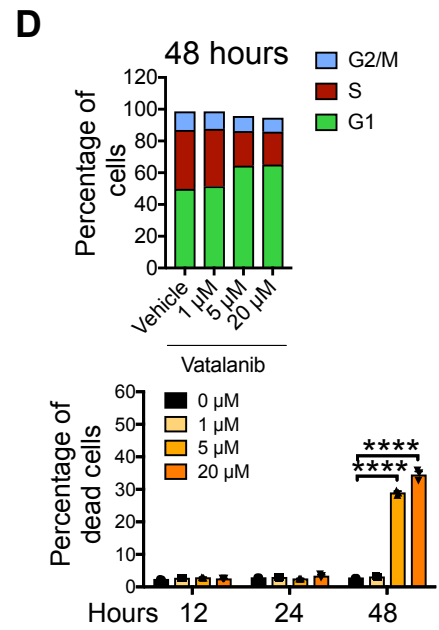
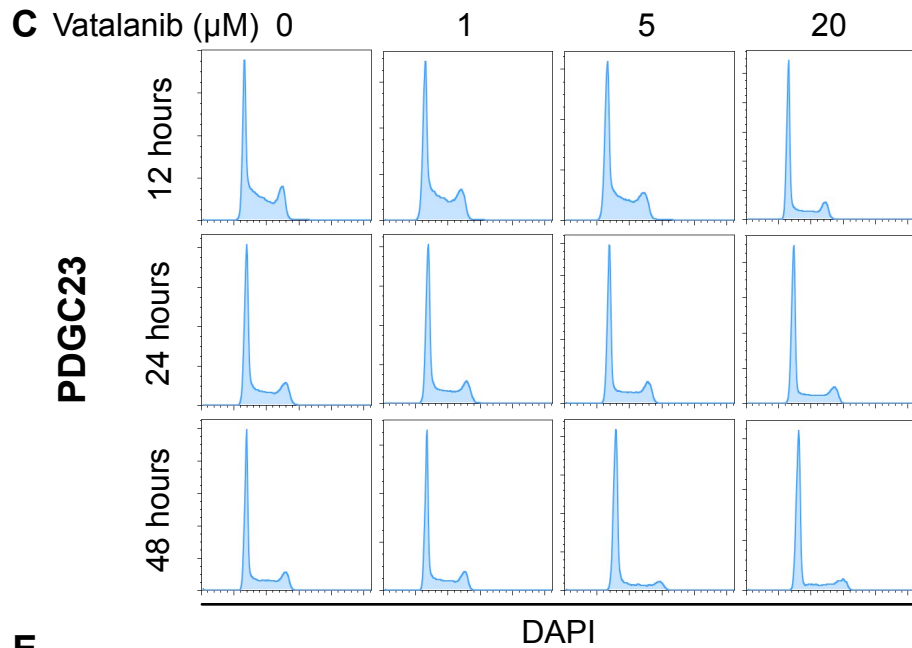
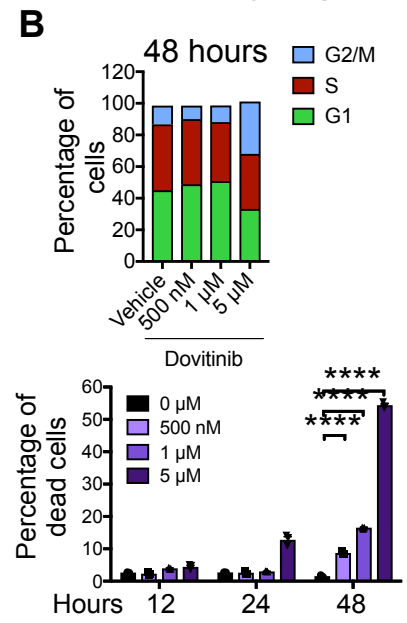
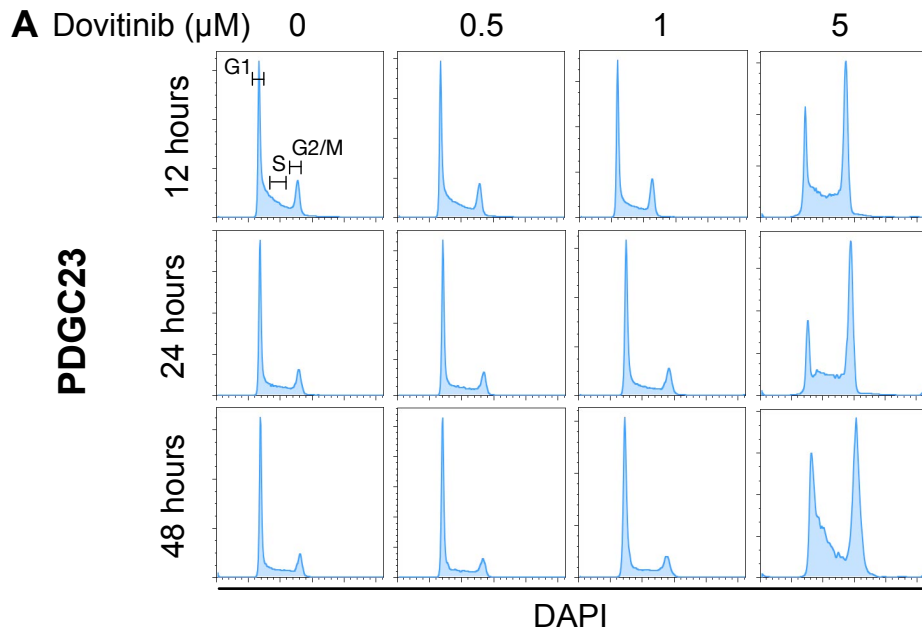
Supplementary Figure 1. Intratumoral expression of receptor tyrosine kinases and on-target inhibition *in vivo*. **(A)** Co-localization of VEGFR2 and CD31⁺ endothelial cells in PDG tumors. **(B)** Expression pattern of c-Kit staining showing overlap with CD31⁺ endothelial cells and CD31⁻ CD68⁻ tumor cells. Scale bars in panels A and B: 20 μ m. **(C)** Pharmacokinetic analysis of PLX3397, vatalanib and dovitinib. Mouse plasma and brain samples (from non-tumor-bearing mice) were analyzed to determine compound concentration 2 hours after dosing, n=3 mice. **(D)** Representative immunoblots of phosphorylated CSF-1R, phosphorylated PDGFR- α and respective total receptors using fractionated whole tumor lysates from animals treated with indicated inhibitors. Densitometry analysis in the right panels shows inhibition of CSF-1R by PLX3397 and inhibition of PDGFR- α by vatalanib and dovitinib, n=3 tumors for each group. The effect of PLX3397 on PDGFR- α phosphorylation could not be assessed due to very low numbers of PDGFR- α -positive tumor cells in the efficiently-debulked gliomas of this treatment group. One-way ANOVA with Sidak's multiple comparisons test was used to calculate statistical significance. * $P < 0.05$; *** $P < 0.001$; **** $P < 0.0001$.



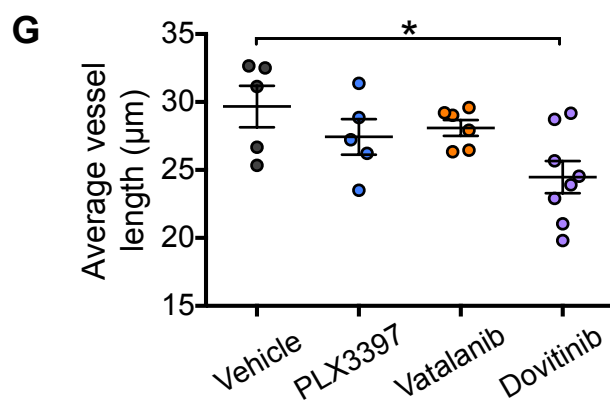
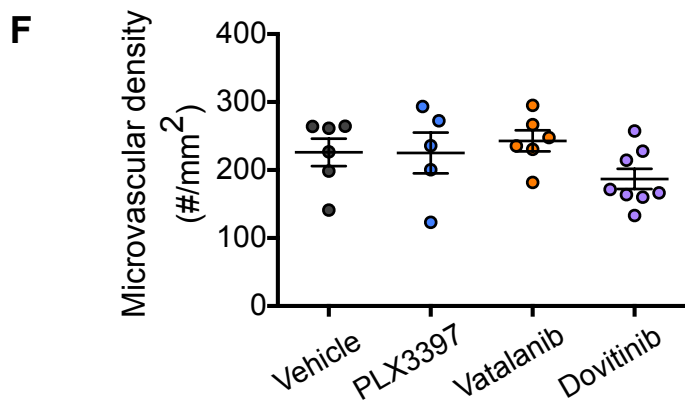
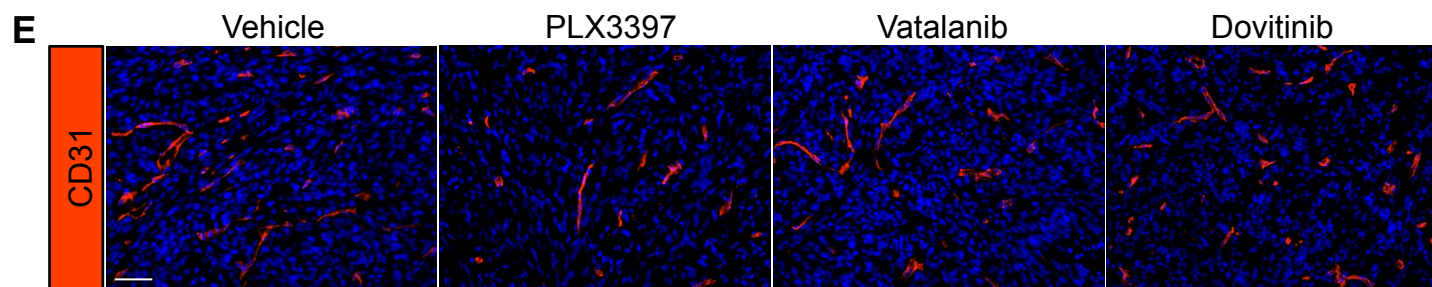
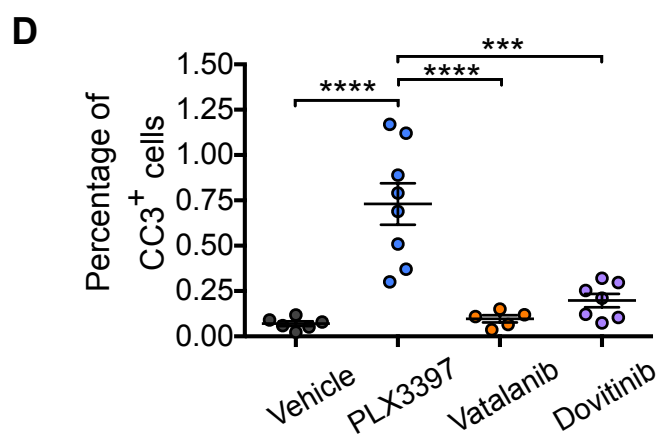
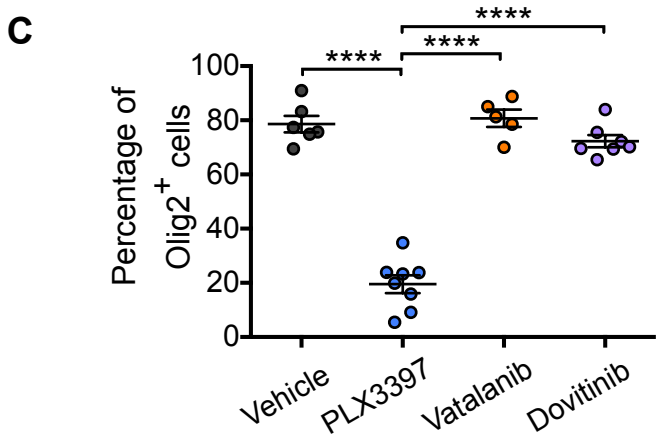
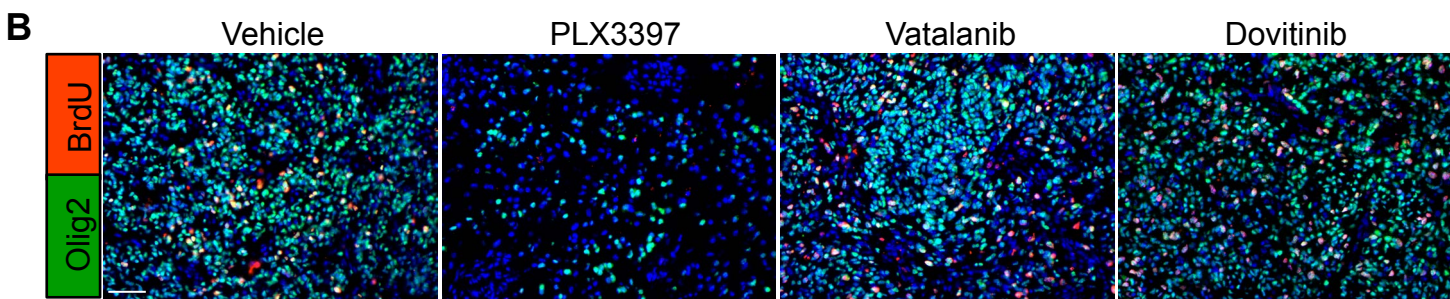
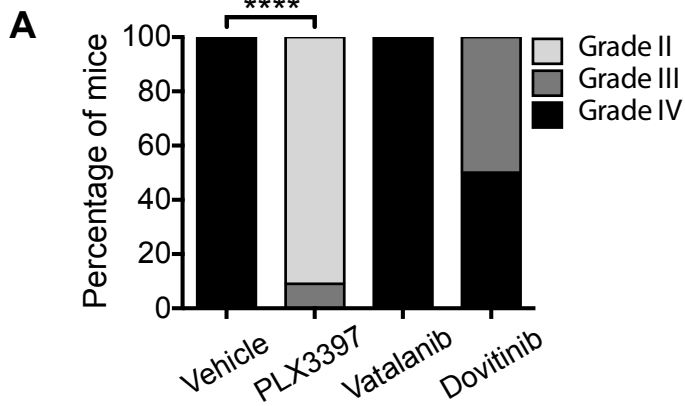
Supplementary Figure 2. On-target inhibition of receptor tyrosine kinases *in vitro*. **(A)** Dose-response curves of murine PDGC23 cells (upper part) and human U-87MG cells (lower part) treated with PLX3397, vatalanib and dovitinib, in serum-free media as assessed using MTT assays. Gray dashed line indicates cellular IC₅₀ and red dashed line denotes physiological compound concentration in the brain parenchyma determined by pharmacokinetic analysis. Graphs depict a representative experiment from a minimum of 4 independent assays. **(B)** MTT assay showing the dose-response relationship between vatalanib or dovitinib and PDGC23 viability, in the presence of PDGF-BB (1 ng/mL). **(C)** Dose-response curves of murine bone marrow-derived macrophages (BMDMs) and human monocyte-derived macrophages (MDMs) treated with PLX3397, vatalanib or dovitinib in the presence of CSF-1 (10 ng/mL), with the gray dashed line indicating cellular IC₅₀ and the red dashed line denoting physiological compound concentration in the brain parenchyma. Graphs depict a representative experiment from 6 independent experiments for both cell types.



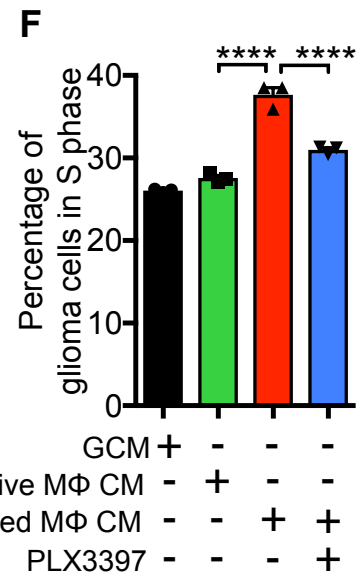
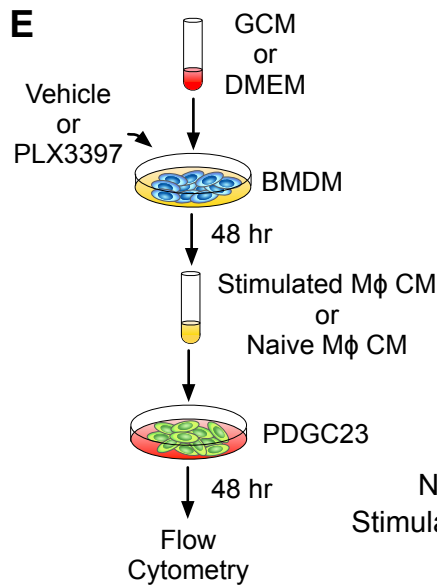
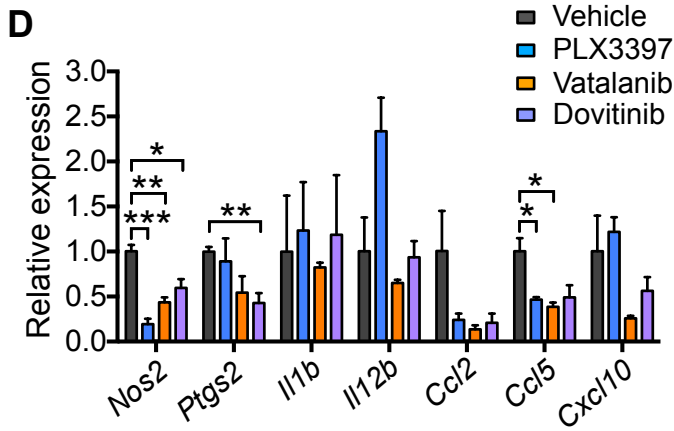
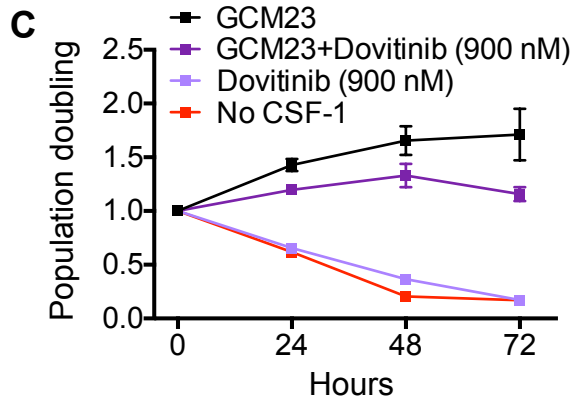
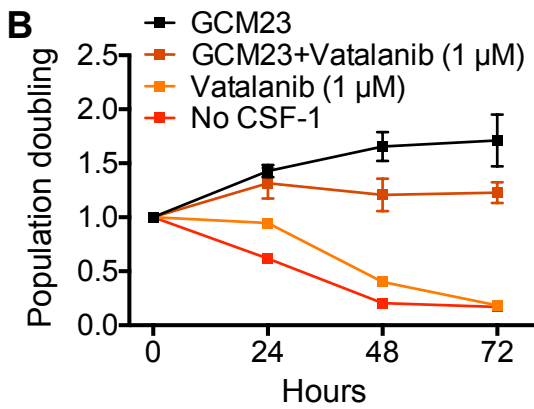
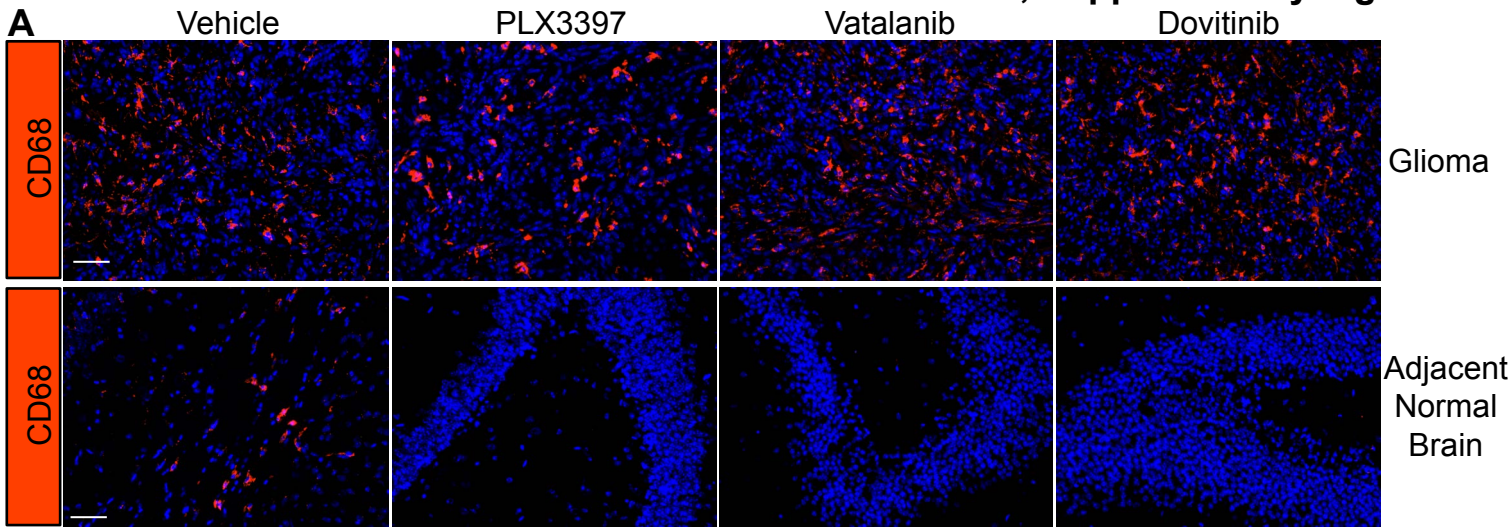
Supplementary Figure 3. Analysis of CSF-1R phosphorylation in the presence of receptor tyrosine kinase inhibitors. Representative immunoblot of phosphorylated CSF-1R and total CSF-1R using lysates from (A) murine BMDMs and (B) human MDMs. Cells were cultured in the absence of CSF-1 for 12 hours and pre-treated with inhibitors: PLX3397 (70 nM or 500 nM, respectively), vatalanib (500 nM) and dovitinib (900 nM or 500 nM, respectively) for 1 hour, and then stimulated with CSF-1 (10 ng/mL) for 5 minutes. Graphs depict the quantification of 3 (BMDMs) and 5 (MDMs) independent experiments. For (A), paired t-test was used to assess statistical significance and for (B) one-way ANOVA with Dunnett's multiple comparison test was used to calculate statistical significance. * $P < 0.05$; *** $P < 0.001$; **** $P < 0.0001$.



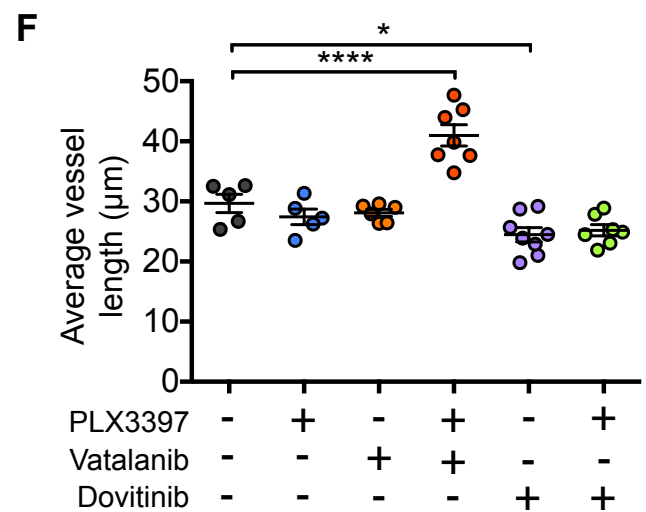
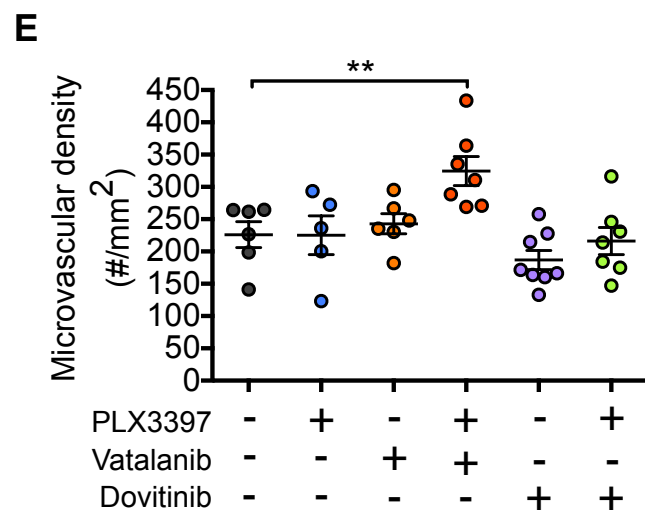
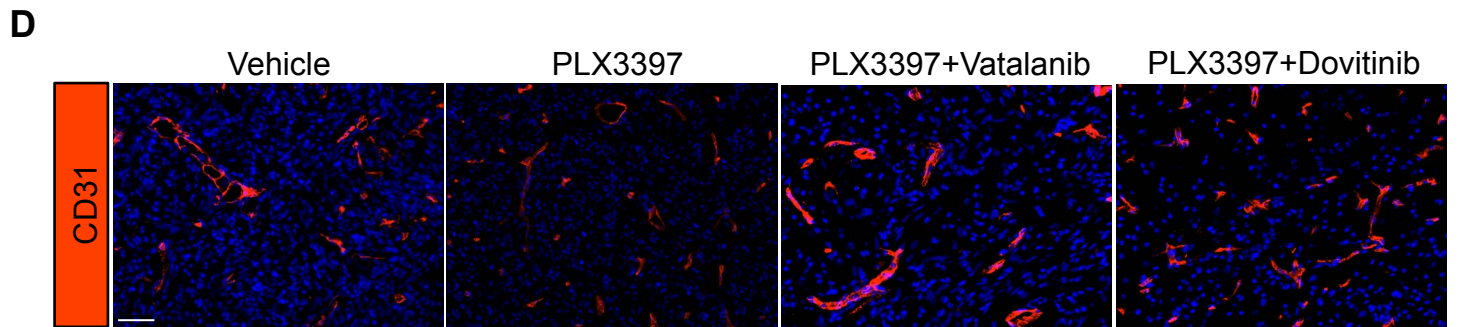
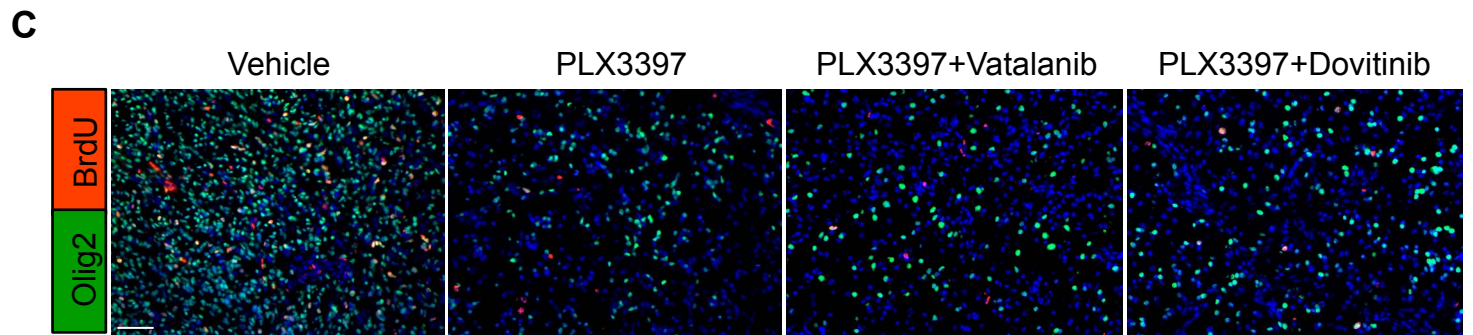
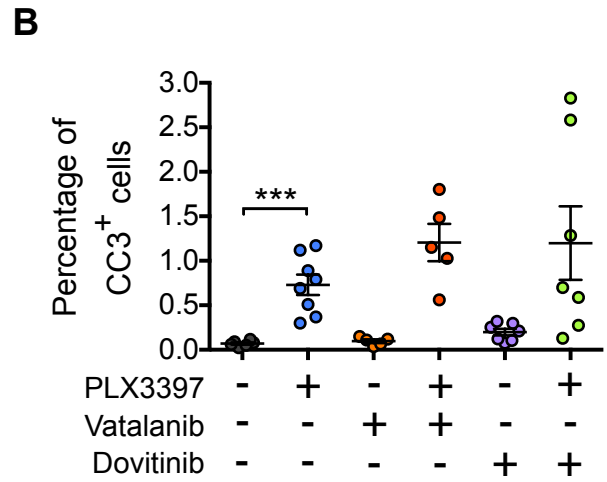
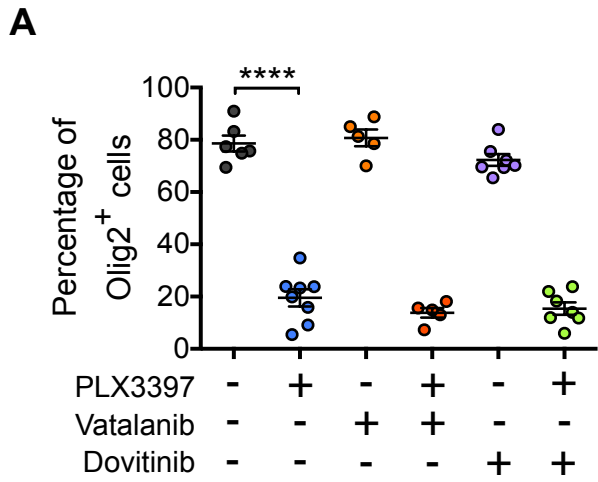
Supplementary Figure 4. Perturbations of cell cycle and cell viability by receptor tyrosine kinase inhibitors. **(A)** Cell cycle analysis of dovitinib-treated murine PDGC23 cells at 12-hour, 24-hour and 48-hour time points. **(B)** Quantification of the percentage of cells in each of phase of cell cycle at 48h (upper panel) and dead glioma cells (APC-Cy7⁺) after 12-hour, 24-hour and 48-hour incubation with dovitinib (500 nM, 1 μ M, 5 μ M) (bottom panel), n=3 independent experiments. **(C)** Cell cycle analysis of vatalanib-treated PDGC23 cells at 12-hour, 24-hour and 48-hour time points. **(D)** Quantification of the percentage of cells in each of phase of cell cycle at 48h (upper panel) and dead glioma cells (APC-Cy7⁺) (bottom panel) after 12-hour, 24-hour and 48-hour incubation with vatalanib (1 μ M, 5 μ M, 20 μ M), n=3 independent experiments. **(E)** Cell cycle analysis of dovitinib-treated U-87MG cells at the 48-hour time point, **(F)** Cell cycle analysis of vatalanib-treated U-87MG cells at the 48-hour time point. For B, D, E and F: individual points represent independent experiments. For B, D, E, F: One-way ANOVA with Dunnett's multiple comparisons test was used to calculate statistical significance, **** $P < 0.0001$.



Supplementary Figure 5. Analysis of alterations in tumorigenic processes within treated gliomas. (A) Composition of tumor grades in all treatment arms, based on the 2007 WHO criteria. Chi-square test was used for statistical comparisons. (B) Representative immunofluorescence images of glioma cell proliferation, with glioma cells labeled by Olig2 positivity and proliferation indicated by BrdU positivity. (C) Quantification of percentages of Olig2⁺ tumor cells. (D) Quantification of percentages of CC3⁺ apoptotic cells within gliomas. (E) Representative immunofluorescence images of intratumoral CD31⁺ vasculature. (F) Quantification of microvascular density within gliomas. (G) Quantification of blood vessel length within gliomas. One-way ANOVA with Sidak's multiple comparisons test and Dunnett's multiple comparisons test were used to assess statistical significance in (C-D) and (F-G) respectively. * $P < 0.05$; **** $P < 0.0001$. Scale bars in panels B and E: 50 μm . For C, D, F and G each point represents an independent tumor.

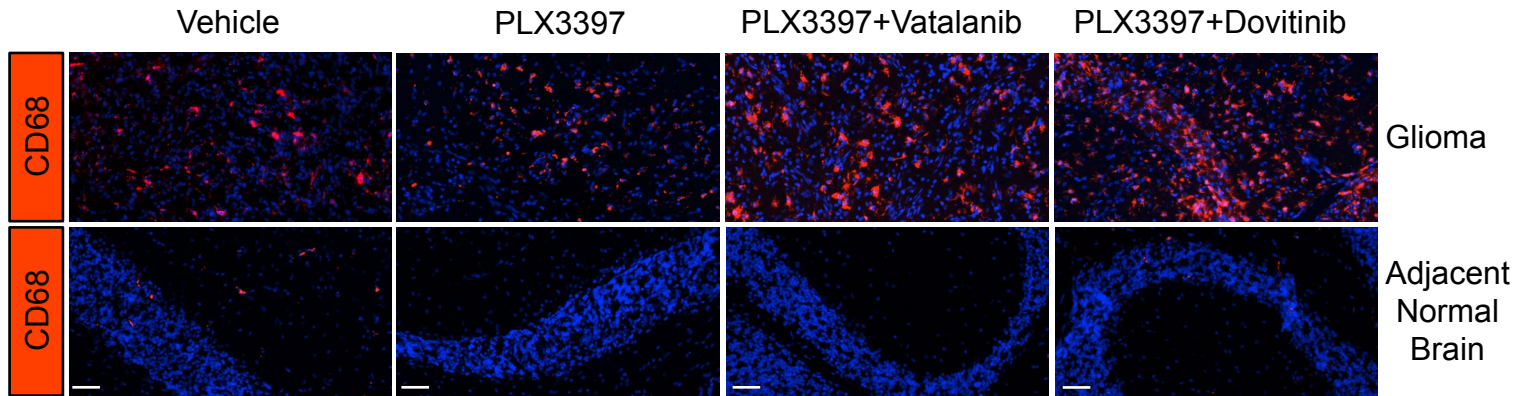


Supplementary Figure 6. Macrophage protection by glioma cell-derived factors and PLX3397-mediated TAM gene expression changes. (A) Representative immunofluorescence images of CD68⁺ TAMs (upper row) and microglia in adjacent normal brain (lower row). Scale bars: 50 μ m. (B) MTT assay showing cell viability of murine BMDMs treated with GCM, vatalanib (1 μ M, based on 2-fold of estimated IC₅₀ from dose-response studies), or a combination of both, n=3 independent experiments. (C) MTT assay showing cell viability of BMDMs treated with GCM, dovitinib (900 nM, based on estimated IC₅₀ from dose-response studies), or a combination of both, n=3 independent experiments. (D) Quantification of mRNA expression of M1-like genes, including *Nos2*, *Ptgs2*, *Il1b*, *Il12b*, *Ccl2*, *Ccl5* and *Cxcl10*, in treated gliomas, n=3 tumors for each group. (E) Schematic of conditioned media cell culture assay. (F) Quantification of proportion of glioma cells in S phase, after incubation with naïve or stimulated M Φ CM generated from BMDMs treated with vehicle (DMSO) or PLX3397 (60 nM), n=3 independent experiments. One-way ANOVA with Sidak's multiple comparisons test and Tukey's multiple comparisons test were used to assess statistical significance in (D) and (E) respectively. * $P < 0.05$; ** $P < 0.01$; *** $P < 0.001$; **** $P < 0.0001$.

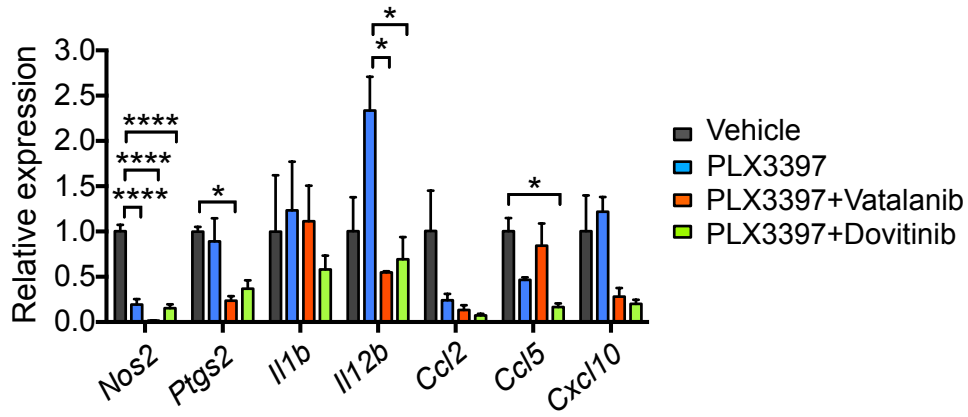


Supplementary Figure 7. Intratumoral changes following administration of combination therapies. (A) Quantification of percentages of Olig2⁺ tumor cells in the different treatment arms. (B) Quantification of percentages of CC3⁺ apoptotic cells. Values in the single-agent groups are from Supplementary Fig. 4C-D for comparison purposes. (C) Representative immunofluorescence images of glioma cell proliferation. (D) Representative immunofluorescence images showing intratumoral vasculature. Scale bars in panels C and D: 50 μ m. (E) Quantification of intratumoral microvascular density in the different treatment arms. (F) Quantification of intratumoral blood vessel length. Values in the single-agent groups are from Supplementary Fig. 4F-G for comparison purposes. One-way ANOVA with Sidak's multiple comparisons test and Dunnett's multiple comparisons test were used to assess statistical significance in (A-B) and (E-F) respectively. * $P < 0.05$; ** $P < 0.01$; **** $P < 0.0001$; n.s. not significant. For A, B, E and F each dot represents an independent tumor.

A



B



Supplementary Figure 8. Gene expression changes in TAMs after combination therapies. (A) Representative immunofluorescence images of CD68⁺ TAMs in the different treatment arms. Scale bar: 50 μ m. (B) Quantification of mRNA expression of M1-like genes, including *Nos2*, *Ptgs2*, *Il1b*, *Il12b*, *Ccl2*, *Ccl5* and *Cxcl10*, in treated gliomas, n=3 tumors for each group. One-way ANOVA with Sidak's multiple comparisons test was used to calculate statistical significance. * $P < 0.05$; ** $P < 0.01$; *** $P < 0.001$.

Supplementary Table 1: List of antibodies used for immunofluorescence (IF) and Western blotting (WB)

Antibody	Clone	Vendor	Dilution
BrdU	BU1/75(ICR1)	Serotec	IF 1:200
c-Kit	D13A2	Cell Signaling Technology	IF 1:400
Cleaved caspase 3 (CC3)	-	Cell Signaling Technology	IF 1:500
CD31	-	R&D Systems	IF 1:100
CD68	FA-11	Serotec	IF 1:1000
CSF-1R	C-20	Santa Cruz	WB 1:1000
Phospho-CSF-1R (Y723)	49C10	Cell Signaling Technology	WB 1:1000
Olig2	-	Millipore	IF 1:200
PDGFR alpha	D1E1E	Cell Signaling Technology	WB 1:1000
Phospho-PDGFR alpha (Y762)	-	Cell Signaling Technology	WB 1:1000
VEGFR2	D5B1	Cell Signaling Technology	IF 1:400